Available online at www.sciencedirect.com
ScienceDirect
International Journal of Heat and Mass Transfer 51 (2008) 52–67
International Journal of HEAT and MASS TRANSFER
www.elsevier.com/locate/ijhmt

Heat transfer and pressure drop properties of high viscous solutions in plate heat exchangers

F.S.K. Warnakulasuriya, W.M. Worek *

Department of Mechanical and Industrial Engineering, University of Illinois at Chicago, Chicago, IL 60607, USA

Received 24 August 2006
Available online 23 October 2007

Abstract

Heat transfer and pressure drop characteristics of an absorbent salt solution in a commercial plate heat exchanger serving as a solution sub-cooler in the high loop of triple-effect absorption refrigeration cycle was investigated. The main objectives of this research were to establish the correlation equations to predict the heat transfer and pressure drop and to analyze and optimize the operating parameters for use in the design of absorption systems.

In order to conduct above studies, a single-pass cross-corrugated ALFA-LAVAL plate heat exchanger, Model PO1-VG, with capacity of 14,650 W (50,000 Btu/h) was used. In order to evaluate the performance, hot solution inlet temperatures from 55 °C (130 °F) to 77 °C (170 °F), and inlet temperature differences from 14 °C (25 °F) to 20 °C (35 °F) were used. The cold side of the heat exchanger was operated to match the equal heat capacity rate of hot side.

Based on the empirical models proposed in the literature, a program was developed and experimental data were curve fitted. From the best-fitted curves, the power-law equations for heat transfer and pressure losses were established and the performance was evaluated.

In the hot salt solution side, the Reynolds number was varied from 250 to 1100 and the resulting Nusselt number varied from 7.4 to 15.8. The measured overall heat transfer coefficient $U_{overall}$ varied from 970 W/m^2 °C (170 Btu/h ft^2 °F) to 2270 W/m^2 °C (400 Btu/h ft^2 °F) and the Fanning friction factor in the absorbent side of the heat exchanger varied from 5.7 to 7.6. The correlation equations developed to predict the heat transfer and friction factor perfectly agree with the experimental results. Those equations can be used to predict the performance of any solution with Prandtl numbers between 82 and 174, for heat exchangers with similar geometry.

Keywords: Absorption refrigeration; Plate heat exchangers; Highly viscous flows in heat exchangers; Power-law equation

1. Introduction

In multi-effect absorption machines, the equipment size is controlled by the mass and heat transfer rates in the high stage absorber. Previous studies have shown that the limiting mechanism in the absorption process is mainly chemical diffusion and heat transfer [1–4]. It is obvious that enhancement of the absorption process reduces the physical size and weight of the overall absorber and lowers the overall power consumption of the system.

The spray absorption process is an adiabatic process. Therefore using a spray absorber to enhance the mass transfer rates as compared to a conventional absorber requires the addition of an external heat exchanger (sub-cooler), as is illustrated in Fig. 1. To optimize the size of the unit, characterizing and optimizing the sub-cooler is important to successfully implement the spray absorption concept. In this work, a commercially available plate heat exchanger with an absorbent salt solution LZB™, supplied by Trane Company, as the heat transfer fluid is used for investigation.

The main objectives of this work are to specify the best suited heat exchanger configuration, define the optimum operating conditions, and to discuss the advantages and

* Corresponding author.
E-mail address: wworek@uic.edu (W.M. Worek).

0017-9310/$ - see front matter © 2007 Elsevier Ltd. All rights reserved.
doi:10.1016/j.ijheatmasstransfer.2007.04.054

Nomenclature

a	plate thickness, m (in.)
A_C	minimum cross-sectional area of single flow passage, m^2 ($in.^2$)
A_t	total heat transfer surface area, m^2 (ft^2)
A, B, C, D	constant and exponents for correlation equations
C_P	specific heat at constant pressure, J/kg °C (Btu/lbm °F)
D_h	hydraulic diameter based on minimum free flow area, m (in.)
f	Fanning friction factor
F	LMTD correction factor
F_t	heat exchanger fouling factor
G	flow field mass velocity, kg/m^2 s (lbm/ft^2 min)
h	film heat transfer coefficient (h_H or h_C), W/m^2 °C (Btu/h ft^2 °F)
H	internal height of the corrugation, m (in.)
k_F	conductivity of solution, W/m^2 °C (Btu/h ft^2 °F)
k_P	conductivity of plate material, W/m^2 °C (Btu/h ft^2 °F)
L	approximate lateral length, m (ft)
LMTD	log-mean temperature difference, °C (°F)
L_t	total length of flow passages, m (ft)
$\dot{m}$	mass flow rate, kg/s (lbm/min)
n	number of furrows across heat exchanger
Nu	average Nusselt number
p	corrugation pitch, m (in.)
P	wetted perimeter, m (in.)
Pr	Prandtl number
ΔP	pressure drop across the heat exchanger, Pa
Q	heat transfer from specified side, W (Btu/h)
r	experimental results
Re	Reynolds number
ΔT	temperature difference, °C (°F)
U_m	flow stream mean velocity, m/s (ft/min)
U	overall heat transfer coefficient, m/s (ft/min)
U_{X_j}	uncertainty in each measured variable
X_j	experimental parameters

Greek symbols

θ	included angle between corrugation (theta), degree
μ	viscosity, kg/m s (lbm/ft min)
ρ	density of solution, kg/m^3 (lbm/ft^3)
ε_i	small perturbation of the variable X_i

Subscripts

INLET	inlet conditions
MEAN	mean value between inlet and outlet
OUTLET	outlet condition
CAL	calculated results
EXP	experimental results
f	free stream condition
w	wall condition

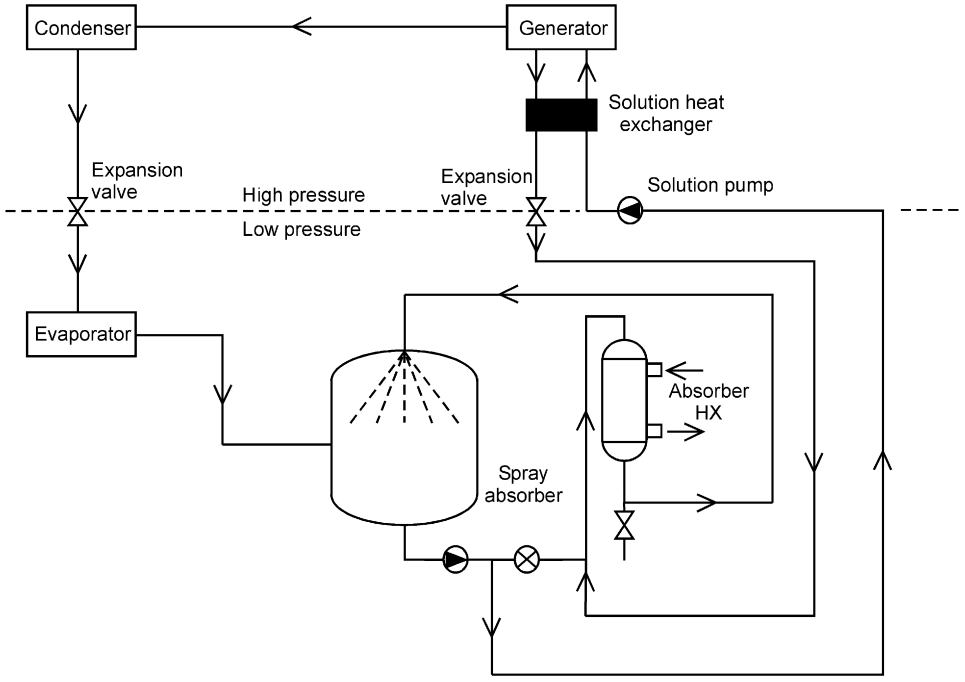

Fig. 1. Spray absorber with solution sub-cooler (HX).

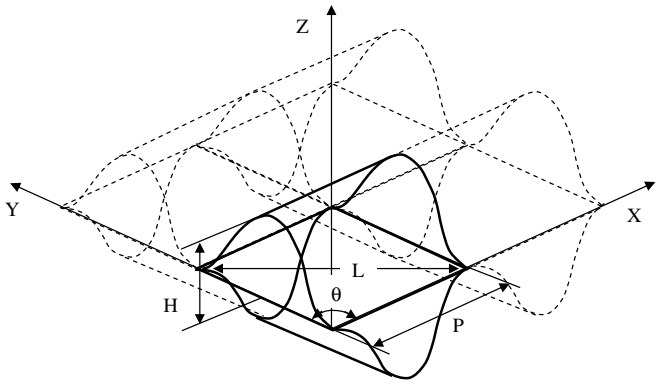

Fig. 2. Unitary cell of heat exchanger.

disadvantages of using a plate heat exchanger as a solution sub-cooler in the high stage of multi-effect spray absorption systems. The differences of optimum conditions, as compared to existing systems, are based on separating the heat and mass transfer processes, the effect of thermal and chemical properties of the salt solution on heat transfer, and pressure drop and its performance under different operating conditions.

Based on the previous studies of Lawry [5], McKillop and Dunkley [6], Troupe et al. [7], Jenson [8], Marriott [9], Cooper [10], Raju and Bansal [11,12] and Edwards [13] on heat transfer in liquid–liquid heat exchangers, a plate type heat exchanger was selected to be used with high viscous and highly temperature dependent solutions. The advantages of using plate heat exchangers with these types of solutions are very significant. Even with highly viscous and low flow rate flows, turbulent or at least swirl can be obtained due to the construction features of the plate heat exchanger

Table 1
Instrument and operating errors

Error source	%	Uncertainty value
Instrument error		
Temperatures (thermocouples)		
Hot inlet temperature		0.12 °C (0.2 °F)
Hot outlet temperature		0.12 °C (0.2 °F)
Cold inlet temperature		0.12 °C (0.2 °F)
Cold outlet temperature		0.12 °C (0.2 °F)
Pressures (gauges)		
Hot side differential pressure	0.1	
Cold side differential pressure	0.1	
Fluid flows (meters)		
Hot side flow	0.2	
Cold side flow	0.2	
Exchanger dimensions		
Corrugation pitch		0.0003 m (0.01 in.)
Internal height of corrugation		0.0003 m (0.01 in.)
Included angle		0.0003 m (0.01 in.)
Operating errors		
Exchanger geometries		
Minimum cross-sectional area		3.3×10^{-6} m^2 (0.005 in.^{2})
Total heat transfer surface area		0.0003 m^2 (0.5 in.^{2})
Exchanger conditions		
Wall temperature		0.67 °C (1.2 °F)
Inlet loss coefficient	4	
Exit loss coefficient	4	
Fouling factor correction	1.5	
Solution properties at mean temperature		
Density	2	
Viscosity	3	
Specific heat	3	
Prandtl number		1.5
Reynolds number		5
Nusselt number		0.12

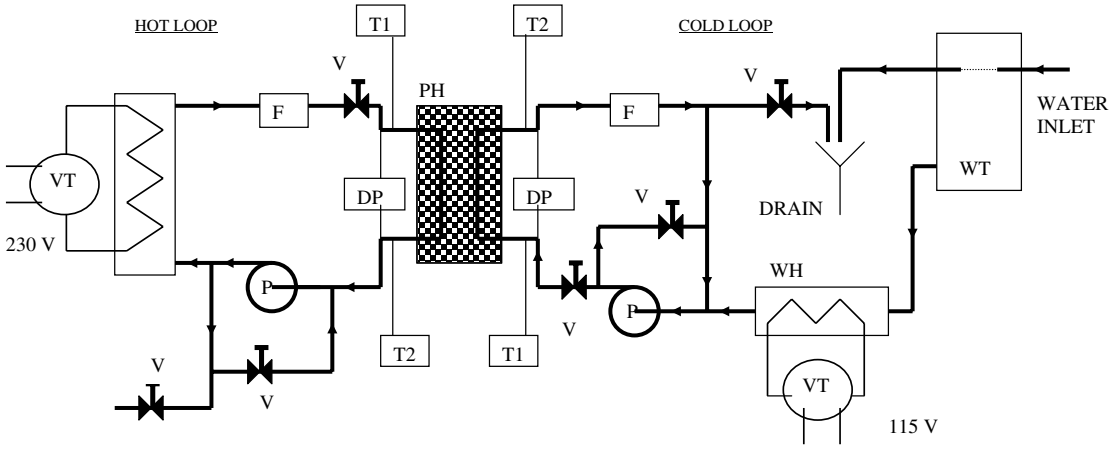

VT	-	VARIABLE TRANSFOMER	DP	-	DIFFERENTIAL PRESSURE TRANSDUCER
FL	-	FLOW METER	T1	-	INLET TEMPERATURE THERMOCOUPLE
P	-	CENTRIFUGAL PUMP	T2	-	OUTLET TEMP THERMOCOUPLE
SH	-	SOLUTION HEATER BANK	WH	-	WATER HEATER BANK
V1	-	FLOW CONTROL VALVE	WT	-	CONSTANT PRESSURE WATER TANK
V2	-	BYPASS VALVE	PHE	-	PLATE HEAT EXCHANGER

Fig. 3. Schematic of the plate heat exchanger test loop.

Table 2
Total uncertainty results

Overall heat transfer coefficient (experimental)	2.0%
Fanning friction factor (experimental)	1.5%
Overall heat transfer coefficient (calculated)	2.25%
Fanning friction factor (calculated)	1.95%

Table 3
Characteristic dimensions of the heat exchanger

Basic dimensions	
Corrugation pitch (p)	0.0102 m (0.40 in.)
Included angle between corrugation (θ)	120°
Internal height of the corrugation (H)	0.0025 m (0.10 in.)
Approximate lateral length (L)	0.0089 m (0.35 in.)
No. of furrows	10
Derived dimensions	
Hydraulic diameter (D_h)	0.0043 m (0.17 in.)
Cross-sectional area (A_C)	2.58×10^{-5} m (0.04 in.^{2})
Wetted perimeter (P)	0.0203 m (0.80 in.)

that enhance the heat transfer. In addition, the ease of assembling and disassembling, the low fouling rate, the ability to operate with any solution (Newtonian and non-Newtonian) and the ability to stand extreme operating conditions, the performance of plate heat exchangers are exceptionally well compared to all other types of heat exchangers.

As outlined earlier, the experiment used in this study was designed to measure the overall performance of the heat exchanger at specified operating conditions. Therefore, based on the above literature, the following assumptions were made to simplify the analyzing of results and to predict the performance:

- Define the overall heat transfer coefficient, $U_{overall}$, based on log-mean temperature difference, LMTD, of the heat exchanger.
- The majority of the heat exchanger flow is hydrodynamically and thermally fully developed.

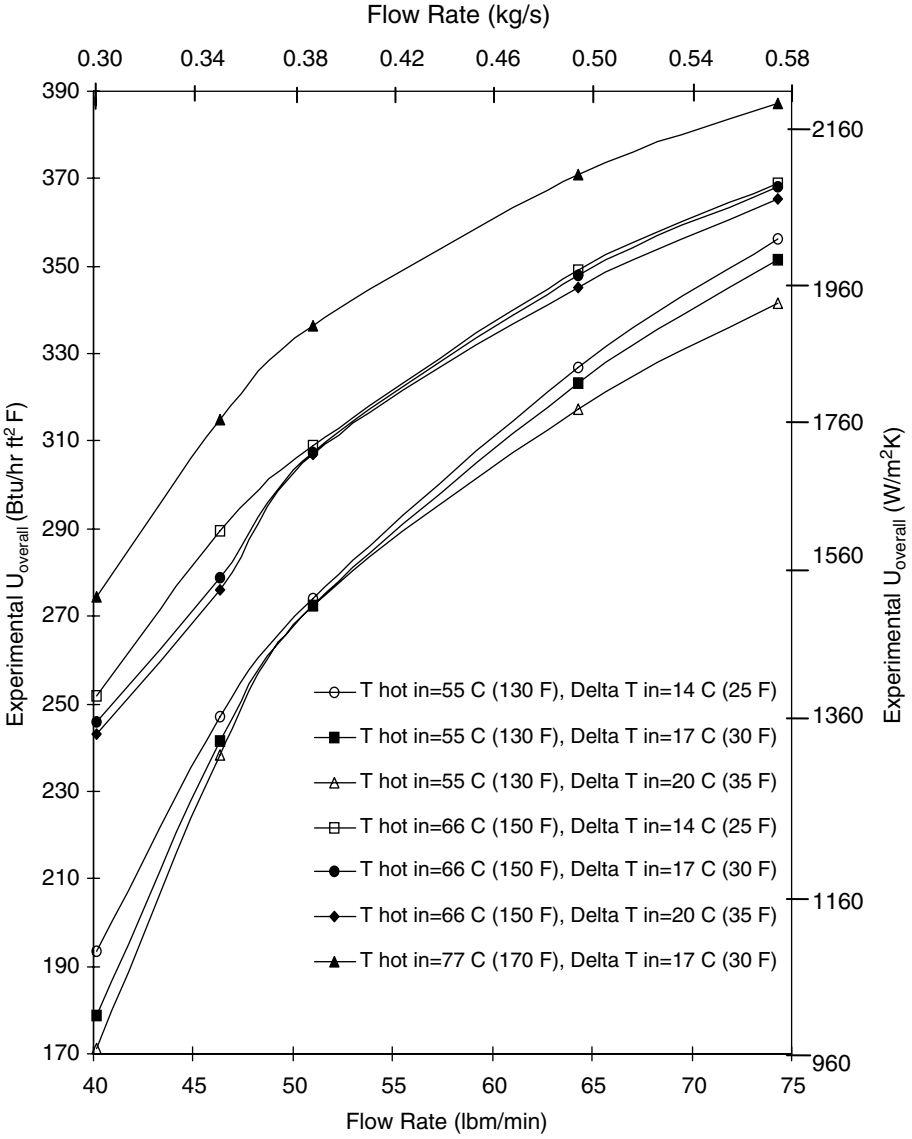

Fig. 4. Experimental overall heat transfer coefficient of solution at different temperatures and different inlet temperature differences.

- Entrance effects and fouling effects are negligible.
- A uniform heat flux (UHF) exists at the boundary between the hot and cold fluid.
- Calculations of mean temperatures are based on inlet and outlet conditions.
- Flow parameters are based on the minimum cross-sectional area in the heat exchanger.

2. Heat transfer coefficient

Based on the above flow conditions and analytical assumptions, the several authors mentioned above have suggested the following equations to calculate the flow and heat transfer performance.

1. When considering fluid properties for calculation based on equal capacity rates, the following equations are used to find the mean temperatures for both hot and cold fluid:

$$\text{Mean fluid temperature} = \frac{T_{\text{IN}} + T_{\text{OUT}}}{2}, \tag{1}$$

$$\text{Mean wall temperature} = \frac{T_{\text{HOT,MEAN}} + T_{\text{COLD,MEAN}}}{2}. \tag{2}$$

2. Based on the assumption of uniform heat flux, the following equation is used to find the heat transfer from each side and hence the overall experimental heat transfer coefficient:

$$Q = \dot{m} C_P \Delta T_{\text{MEAN}}. \tag{3}$$

In addition to Eq. (3), Eq. (4) is used to find overall experimental heat transfer coefficient based on the log-mean temperature difference (LMTD)

$$Q = U_{\text{EXP}} A_{\text{t}} \,\text{LMTD}\, F, \tag{4}$$

where

$$\text{LMTD} = \frac{\Delta T_{\text{INLET}} - \Delta T_{\text{OUTLET}}}{\ln(\Delta T_{\text{INLET}} / \Delta T_{\text{OUTLET}})}. \tag{5}$$

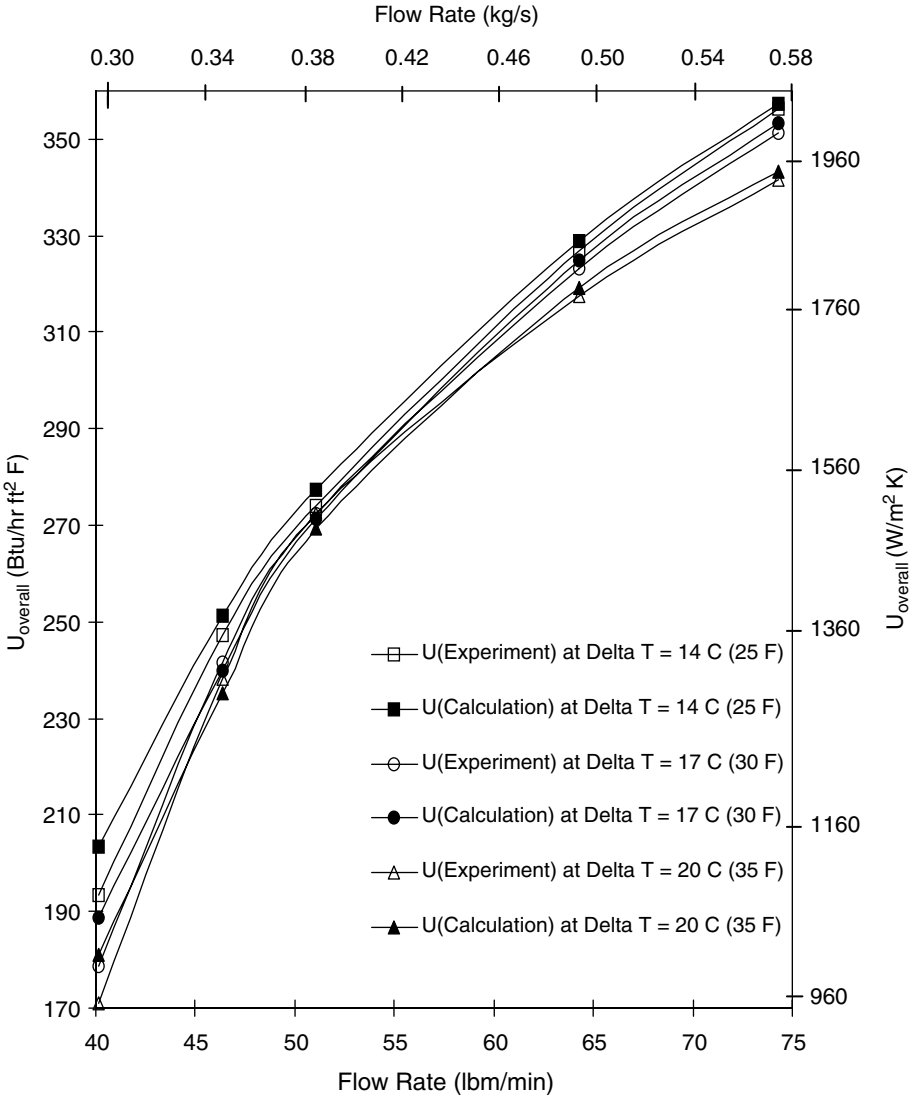

Fig. 5. Curve fitting of overall heat transfer coefficient from high Reynolds turbulent model calculation at 130 °F inlet temperature.

Based on above equations, the overall experimental heat transfer coefficient can be calculated using

$$U_{\mathrm{EXP}} = \frac{\dot{m} C_P \Delta T_{\mathrm{MEAN}}}{A_t \,\mathrm{LMTD}\, F}, \tag{6}$$

where the correction factor F for a single-pass counter-flow heat exchanger is unity.

3. Based on the empirical correlation developed to model the heat exchanger, the Nusselt number and hence film heat transfer coefficient can be found and following equation can be used to obtain the overall calculated heat transfer coefficient:

$$U_{\mathrm{CAL}} = \frac{1}{\frac{1}{h_{\mathrm{H}}} + \frac{1}{h_{\mathrm{C}}} + \frac{a}{k_{\mathrm{P}}} + F_t}, \tag{7}$$

where h_{H} and h_{C} are determined using

$$h = \frac{Nuk_f}{D_h}. \tag{8}$$

4. Based on the heat exchanger plate geometry and measurements, the hydraulic diameter was defined as

$$D_h = \frac{4A_C}{P}. \tag{9}$$

5. When evaluating the cross-sectional area and the perimeter of the flow path in the heat exchanger based on the assumption of sine curve as shown in Fig. 2, Focke et al. [14], Stasiek et al. [15] and Ciofalo et al. [16] suggested to use the following equations:

$$A_C = \frac{3pH \sin(\theta/2)}{2 \sin\theta} \tag{10}$$

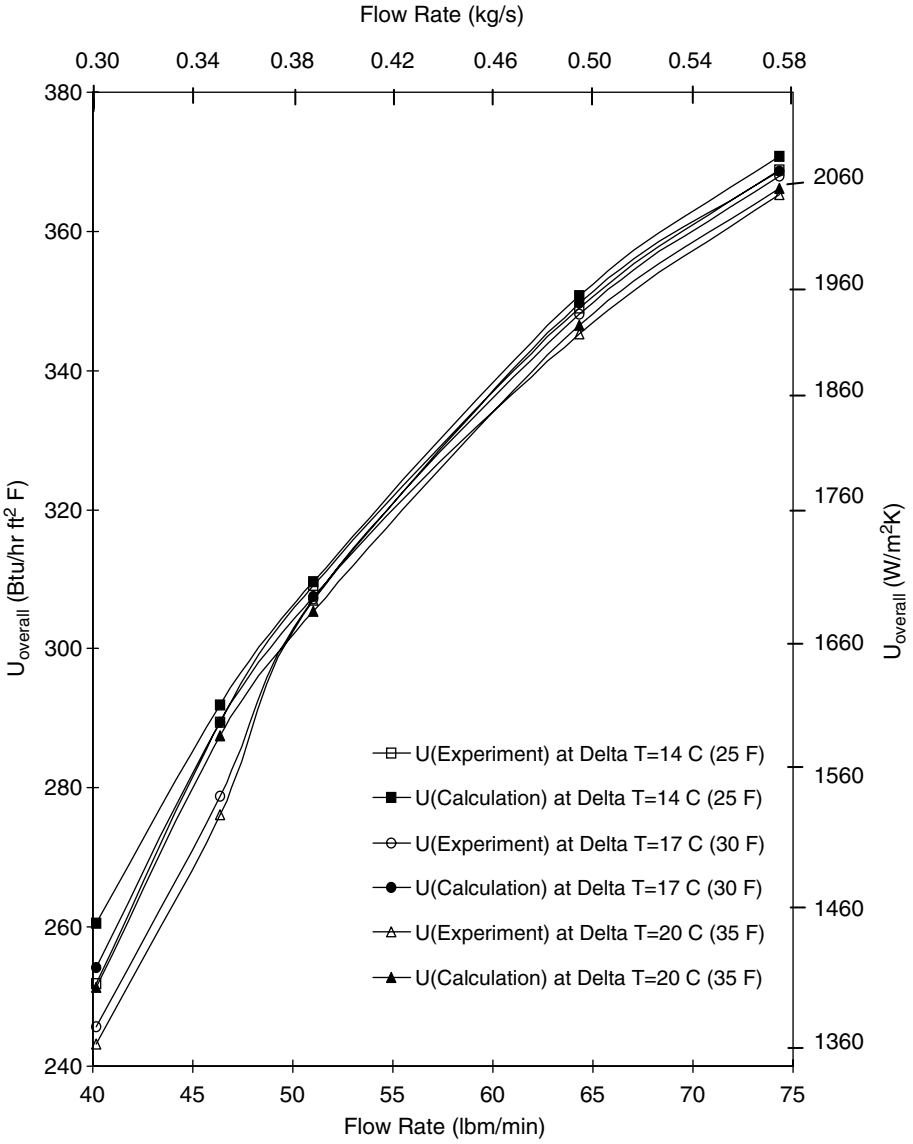

Fig. 6. Curve fitting of overall heat transfer coefficient from high Reynolds turbulent model calculation at 150 °F inlet temperature.

and

$$P = \frac{3L\sin(\theta/2)}{\sin\theta}. \tag{11}$$

To find the film heat transfer coefficients, a conventional approach suggested by Shah and London [17], Kays and Perkins [18], Shah and Bhatti [19], for plate heat exchangers was used. According to McKillop and Dunkley [6], Troupe et al. [7], Buonopane et al. [20], Crozier et al. [21], Marriott [9], Clark [22], Cooper [10] and Edwards [13], this form is specially suited for heat exchangers having complicated geometries and when the properties of the fluids are highly temperature dependent. That is

$$Nu = ARe^{B}Pr^{C}\left(\frac{\mu_f}{\mu_w}\right)^{D}, \tag{12}$$

where

$$Re = \frac{D_h G}{\mu_f} \tag{13}$$

and

$$Pr = \frac{\mu_f C_P}{k_f}. \tag{14}$$

Typical reported values for turbulent flow of the above A, B, C and D constants can be found in the literature. Marriott [9] summarized that these parameters typically are in the following ranges:

$0.15 < A < 0.40,$
$0.65 < B < 0.85,$
$0.30 < C < 0.45,$
$0.05 < D < 0.20.$

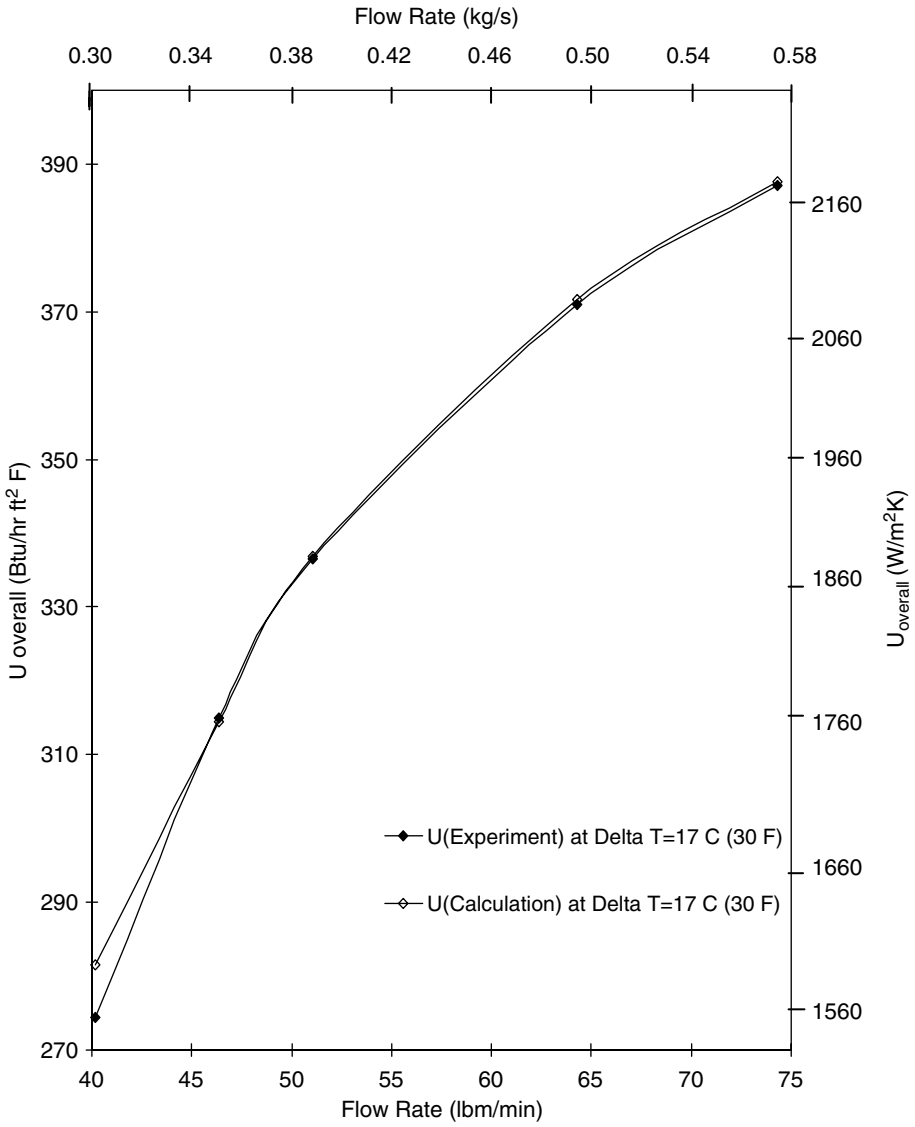

Fig. 7. Curve fitting of overall heat transfer coefficient from high Reynolds turbulent model calculation at 170 °F inlet temperature.

However, in the case of heat transfer coefficient for the turbulent flow with moderate to high Reynolds numbers with small viscosity variations, Buonopane et al. [20] and Cooper [10] showed Eq. (15) fairly accurately predicted the Nusselt number

$$Nu = ARe^{B}Pr^{C}. \tag{15}$$

The flow patterns and the local velocities, which significantly affect on the heat transfer coefficient, are highly dependent on the mass flow rate, the inlet fluid temperature and the temperature difference between the hot and cold fluids. The local velocities within the exchanger, which significantly affect the performance, can be as high as four times the average velocity.

3. Pressure drop

Based on the analysis of heat exchangers, pressure drop is one of the main parameters to consider when designing and operating the heat exchanger in system. Limitation of permissible pressure drops could be based on economic considerations dictated by pumping costs or process limitations or both. The economic design of plate heat exchangers involves complete utilization of the permissible pressure drop while determining the heat transfer area requirement.

In a plate heat exchanger, the pressure drop requirements can be closely met due to the flexibility involved in the choice of plates with respect to their size, configuration, number and the arrangement of flow passes. The extensive analysis

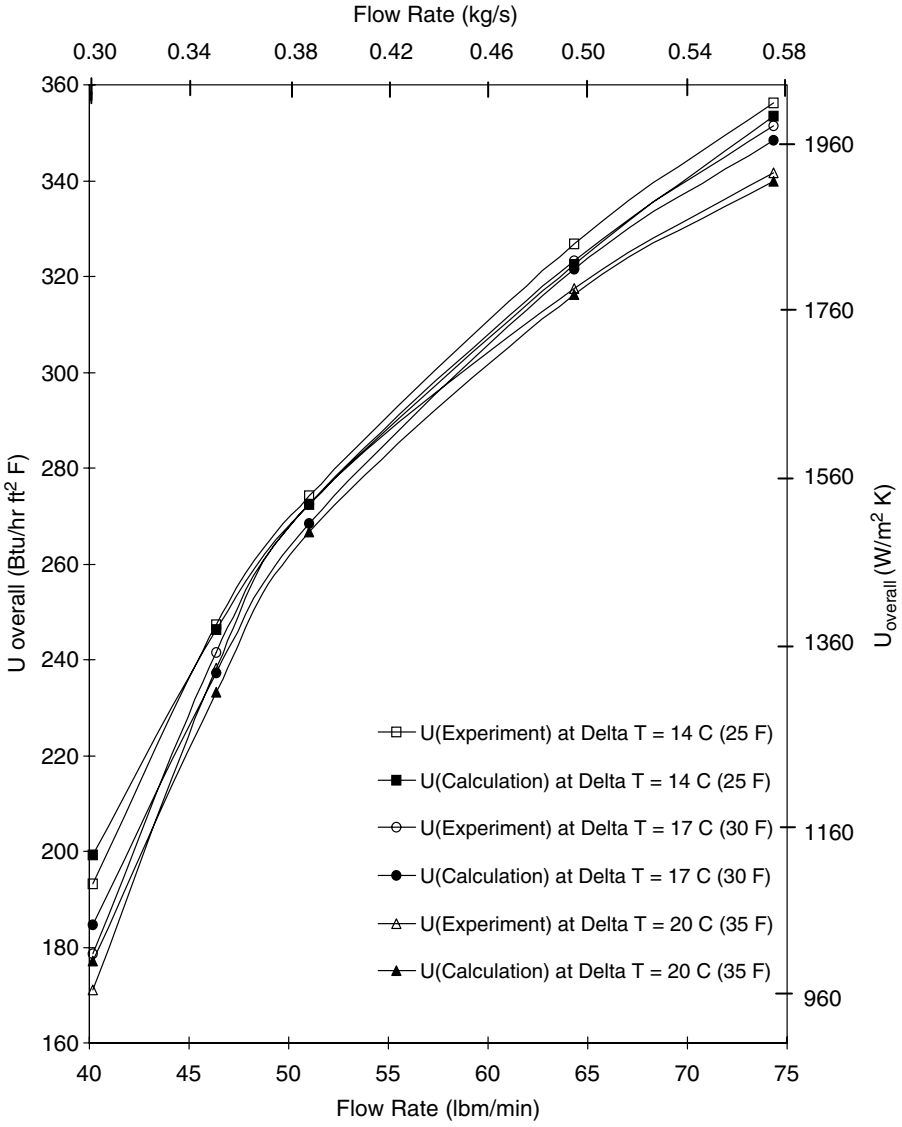

Fig. 8. Curve fitting of overall heat transfer coefficient from low Reynolds turbulent model calculation at 130 °F inlet temperature.

of effects of above factors can be found in Jenson [8], Troupe et al. [7], Marriott [9], Edwards [13] and Cooper [10].

The pressure drop can be correlated by using the Fanning friction factor defined as

$$f = \frac{\Delta P}{\frac{1}{2}\rho U_{\mathrm{m}}^2\left(\frac{L}{D_{\mathrm{h}}}\right)}, \tag{16}$$

where

$$U_{\mathrm{m}} = \frac{\dot{m}}{A_{\mathrm{C}}\rho n}. \tag{17}$$

As defined by Focke et al. [14] and Ciofalo et al. [16], finding the exact total length of flow passages is a difficult task. Considering the suggestion of replacing the length to hydraulic diameter ratio with the area ratio as suggested by Kays and London [23] removes this problem

$$\frac{L_{\mathrm{t}}}{D_{\mathrm{h}}} = \frac{A}{4A_{\mathrm{C}}}. \tag{18}$$

As given by Raju and Bansal [11,12], Edwards [13] and Focke et al. [14], two general empirical correlations are used to find the dependence of the experimental friction factor on the Reynolds number and flow conditions. The general form of empirical equation for turbulent flow in a plate heat exchanger is given as

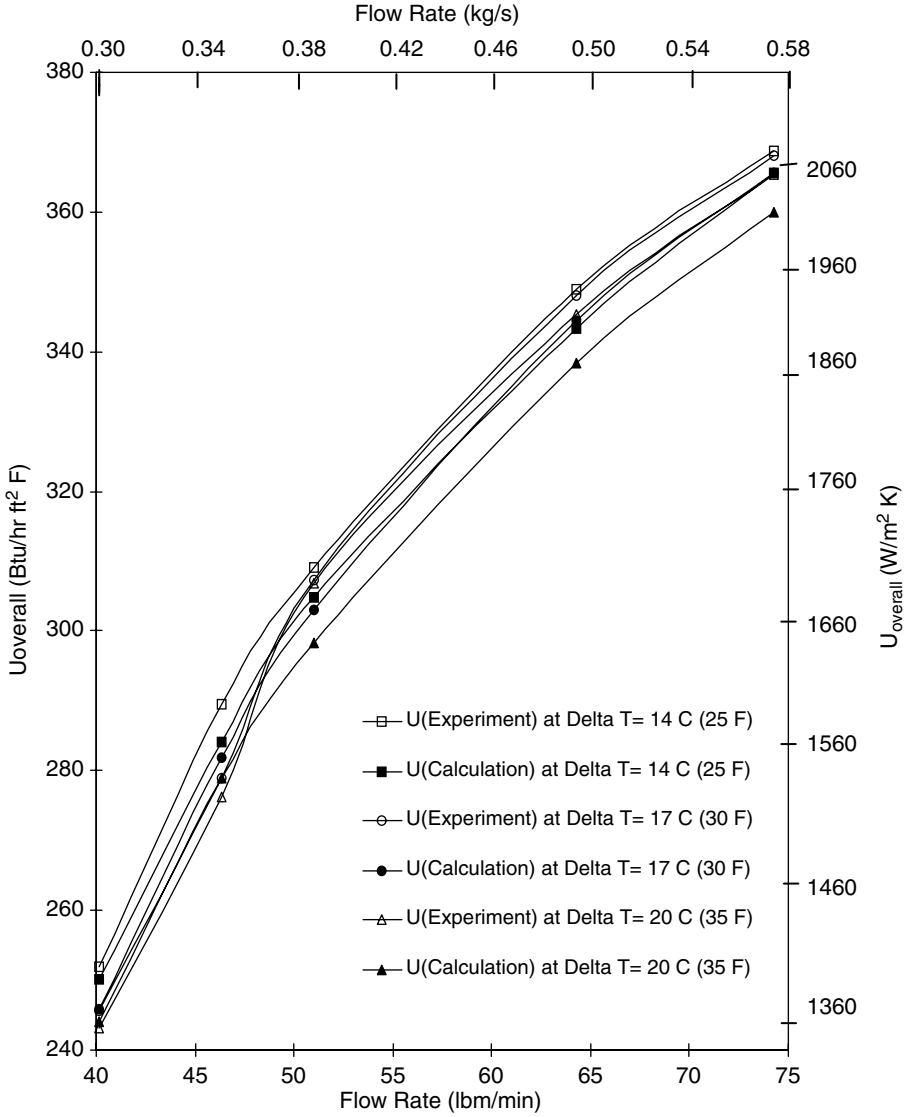

Fig. 9. Curve fitting of overall heat transfer coefficient from low Reynolds turbulent model calculation at 150 °F inlet temperature.

$$f = \frac{A}{Re^B}. \tag{19}$$

Typical reported values for A and B are highly variable and are heavily depends on the corrugation angle, Re number and Pr number as found in Focke et al. [14].

4. Experimental design

When selecting the equipment and instruments, and constructing the experimental test stand for heat transfer testing, the following factors were considered:

- physical size and capacities of the units;
- flow pattern and geometry of the heat exchanger;
- compatibility with the salt solution;
- ease of assembly and disassembly;
- ease of charging and discharging the system and
- repeatability for continuous operation.

Based on above considerations, an ALFA-LAVAL model PO1-VG cross-flow cross-corrugated plate heat exchanger was selected.

A test loop was designed and constructed to accommodate the heat exchanger with capacity of 14,650 W (50,000 Btu/h). The maximum hot side temperature was 77 °C (170 °F) with the corresponding flow rate of 0.61 kg/s (80 lbm/min), and the maximum cold side temperature was 63 °C (145 °F) and flow rate of 0.23 kg/s (30 lbm/min).

For illustration purposes, the experimental setup is basically divided to four sub systems, namely the heat exchanger, the hot loop, the cold loop and the control and data acquisition system. The schematic diagram of the heat transfer test setup is shown in Fig. 3.

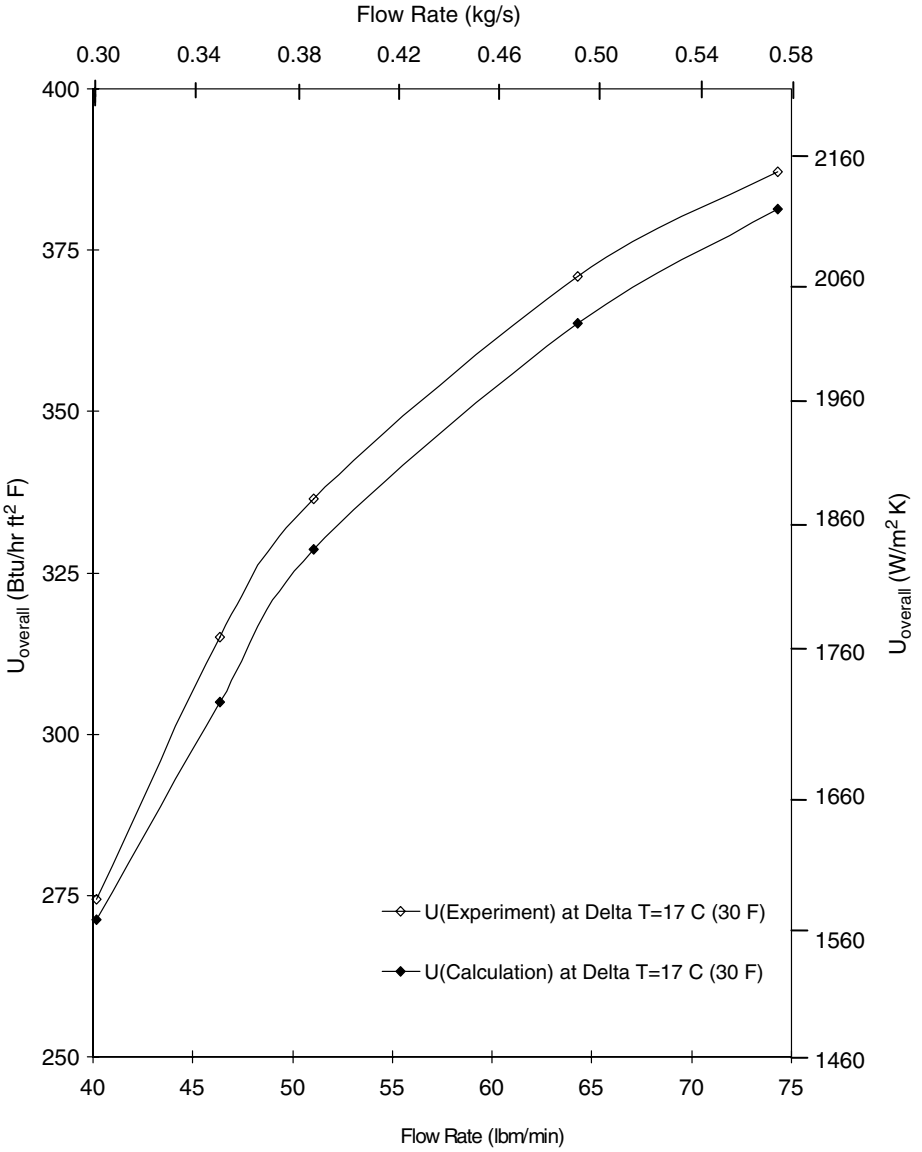

Fig. 10. Curve fitting of overall heat transfer coefficient from low Reynolds turbulent model calculation at 170 °F inlet temperature.

5. Experimental uncertainty analysis

An uncertainty analysis of the experimental performance of the cross-flow heat exchanger will yield the nominal values of the performance parameters (rating, pressure drops, and exit temperatures) as well as the uncertainty in each performance parameter resulting from the uncertainties of the heat transfer surface databases, the stream characteristics, and the physical dimension of the heat exchanger [24]. The affect of the experimental uncertainties of all the measured values influences the overall calculated performance of the system.

The error analysis presumes that all input streams, properties and instrument errors are defined and that the heat exchanger geometry is known. The experimental result is computed using data reduction equation having the general form

$$r = r(X_1, X_2, \ldots, X_j). \tag{20}$$

Each parameter X_i $(i = 1, 2, \ldots, j)$ is one of the j measured variables. The uncertainty of the results is computed to first-order accuracy using the root-sum-square product of the uncertainties in each of the measured variables, U_{X_i}, and the partial derivatives of the results with respect to each of the measured variable. That is,

$$U_r^2 = \left[\frac{\partial r}{\partial X_1} U_{X_1}\right]^2 + \left[\frac{\partial r}{\partial X_2} U_{X_2}\right]^2 + \cdots + \left[\frac{\partial r}{\partial X_j} U_{X_j}\right]^2. \tag{21}$$

Each partial derivative represents the sensitivity of the result to small changes in that variable and was evaluated using the following finite difference approximation:

$$\frac{\partial r}{\partial X_i} = \frac{r(X_1, \ldots, X_i + \varepsilon_i, \ldots, X_j) - r(X_1, \ldots, X_i, \ldots, X_j)}{\varepsilon_i}. \tag{22}$$

When using the above equation for analyze, the value of the ε_i is considered as the large of $X_i/1000$ or 10^{-6}. When determine the uncertainty of operating errors of solution properties and geometry, the relevant equation is used. For inlet, the exit loss coefficient, and the fouling factor, the equations from literature were used [25]. The heat transfer performance, the pressure drop, the exit temperatures, and

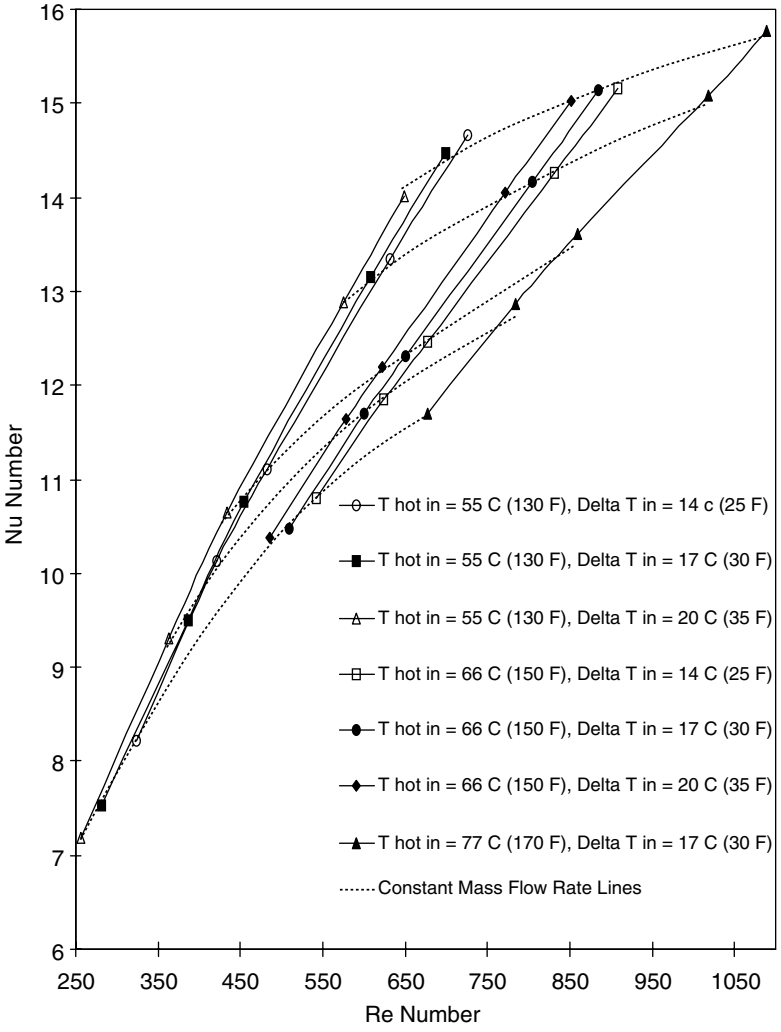

Fig. 11. Variation of Nusselt number with Reynolds number of solution at different inlet temperature and different inlet temperature differences.

the associate errors are summarized in Table 1 and the total uncertainties found for both experimental and calculated results are given in Table 2.

6. Results and discussion

When designing and selecting a heat exchanger, the important parameters are the effectiveness and the overall performance of the device. The effectiveness is a function of the operating temperatures (LMTD) and the heat exchanger geometry. In this discussion, those fundamental quantities that affect the heat transfer and pressure losses will be considered. The basic characteristic length dimension (i.e. equivalent hydraulic diameter) was defined based on the minimum free flow area of the plate heat exchanger. When developing the equations and relations to express the geometry of the heat exchanger, the real geometry of the heat exchanger was closely matched to the corrugated sinusoidal ducts. The measured and calculated characteristic dimensions of the plates of the heat exchanger, as shown in Fig. 2, are given in Table 3. These geometric parameters were obtained using Eqs. (9)–(11).

The experimental results for the overall heat transfer rate for different inlet temperatures with varying inlet temperature differences, based on equal heat capacity rates, are shown in Fig. 4. The experimental results for the overall heat transfer coefficient, U_{overall}, are based on averaging the overall heat transfer coefficients for both the hot and cold sides. These results clearly show the dependence of the heat transfer coefficient on flow rate is more pronounced at low flow rates.

All the basic parameters related to the heat exchanger geometry, fluid properties and flow conditions were determined and the main flow parameters such as Reynolds numbers, Prandtl numbers are calculated and plotted. The results are then curve fitted. From the above plots which are shown in Figs. 5–7, the power-law equation which satisfy the heat exchanger performance is derived as

$$Nu = 0.292 Re^{0.705} Pr^{0.35}. \tag{23}$$

These figures show that the flows with Reynolds number of 400 or more, the calculated U_{overall}, which are based on the above equation closely, matched the experimental results. However, at Reynolds number below 400, the predicted and experimental results deviate considerably.

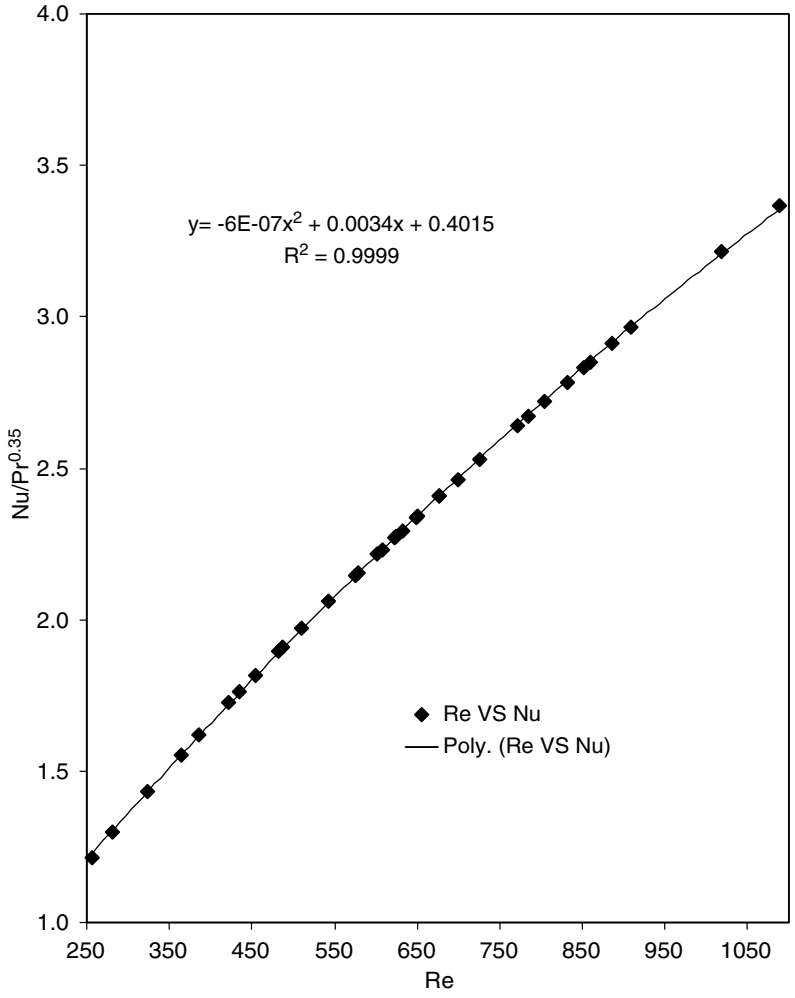

Fig. 12. Effects of Reynolds and Prandtl number on Nusselt number of solution of high Reynolds turbulent model.

Based on these observations, the necessity of the development of a model flow equation that better simulates the low flow range was identified. From the properties and parameters that affect for above deviation, and the experimental data at low flow rates, the effect of viscosity and need for inclusion of a viscosity term in the correlation was identified. The equation that includes viscosity variation was developed (see Eq. (21)). These results are shown in Figs. 8–10

$$Nu = 0.292 Re^{0.705} Pr^{0.35} \left(\frac{\mu_f}{\mu_w}\right)^{0.14}. \quad (24)$$

Figs. 11 and 12 show the effect of Reynolds number and solution flow rate on the Nusselt number and can be used to model the performance of larger heat exchangers. These plots of Nusselt number versus Reynolds number with constant mass flow rate lines and the non-dimensional parameter of $Nu/Pr^{0.35}$ versus the Reynolds number were based on the power-law equation developed for high Reynolds numbers.

When a heat exchanger operates with solutions whose viscosity change dramatically with the operating temperature, many factors need to be considered and special cautions need to be taken. The factors that effect for the performance of heat exchanger under above situation can be explain as: (1) increased flow resistance at the end of the channels closer to outlet due to cooling down the fluid, (2) sedimentary buildups and solidifications at narrow part of flow passages, (3) cold pockets at the end zone away from the main flow paths. Due to above specified reasons, even though the Nusselt number increases with increasing Reynolds number, due to increase of flow rate, when the inlet temperature difference increases, the Reynolds number and hence the Nusselt number decreases, as can be seen in Fig. 11. However, as seen in Figs. 4 and 11, this can be overcome either by increasing the inlet temperature of the solution or decreasing the inlet temperature differences.

Due to this dependency of Nusselt number and Reynolds number on solution flow rate, inlet temperature and inlet temperature differences, defining the optimal flow

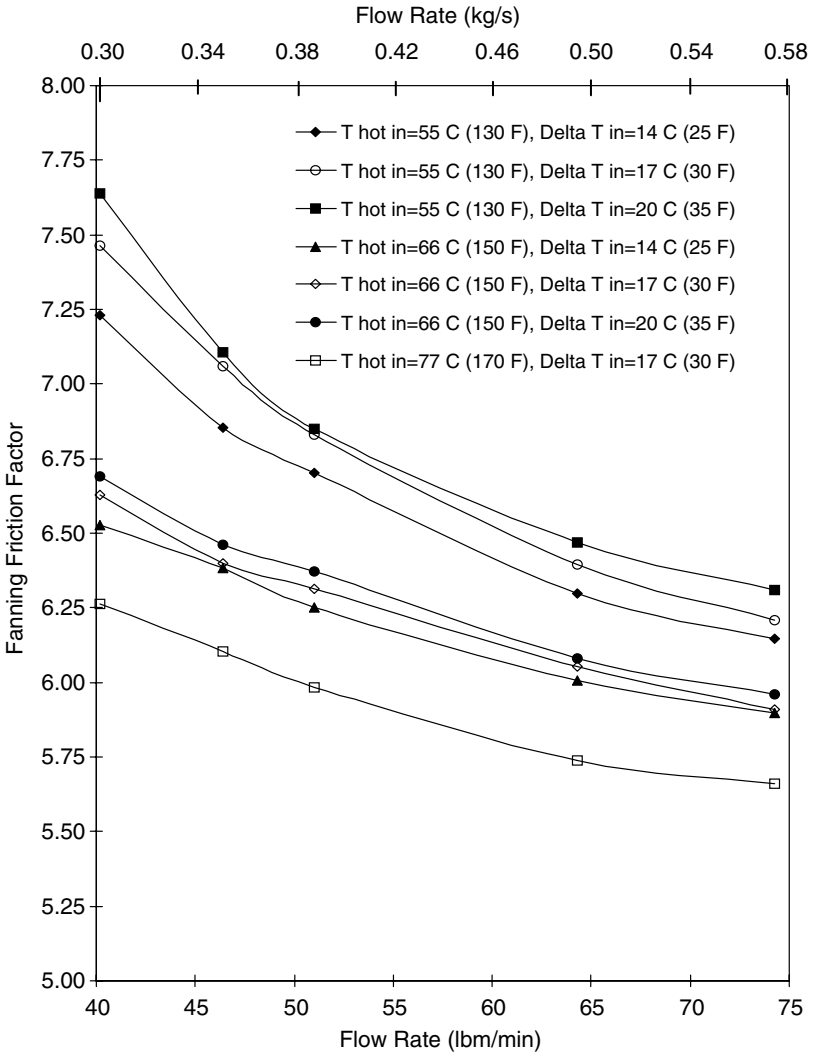

Fig. 13. Fanning friction factor of solution at different inlet temperatures and varying inlet temperature differences.

rate for different operating requirements must be based on both heat transfer and pressure drop calculations.

Comparison of the Nusselt number at two different hot inlet temperatures with the same inlet temperature difference and the same Reynolds number shows a fairly large decrease of the Nusselt at higher temperatures. This reduction of Nusselt number, at the same Reynolds number at higher temperature, is due to the decrease of viscosity and the reduction of flow rate of the solution. Therefore, this drop in Nusselt number does not translates into a similar drop in effectiveness.

Fig. 12 shows that the dependence of $Nu/Pr^{0.35}$ on Reynolds number, that reflect the dependence of the fluid properties to flow condition, collapses all previous data of different hot inlet temperatures onto a single curve. Therefore using this curve, it will be much easier to predict the behavior of the solution and the performance of the heat exchanger.

Using the overall pressure drop obtained experimentally on the heat transfer tests, the Fanning friction factor was determined. These results for the different flow conditions are shown in Figs. 13 and 14. Using the same procedure as was presented previously for heat transfer model, the results were curve fitted. The result, given in Eq. (22) can be used to predict the friction factor and hence pressure drop for cross-corrugated plate heat exchangers using any solution with similar properties as the heat transfer fluid

$$f = 23.8Re^{-0.205}. \tag{25}$$

The above relation closely matches the correlations developed in the literature to predict the Fanning friction factor in the cross-corrugated plate type heat exchangers and the comparison of the experimental results and the calculated results for Fanning friction factor are shown in Fig. 15.

7. Conclusions

The overall heat transfer coefficient and pressure drop in a plate heat exchanger was developed and the experimental results were correlated. From the results in plate heat exchanger investigated in this work, the transition to turbulent flow occurs at Reynolds numbers as low as 10–400. Hence, even at the moderate velocities plate heat exchangers can achieve high heat transfer coefficients, low fouling rates and reduction of overall size. With high heat transfer coefficients, high overall transfer rates can be achieved in comparatively smaller flow paths and thereby keeping the overall size and pressure drop at the minimum.

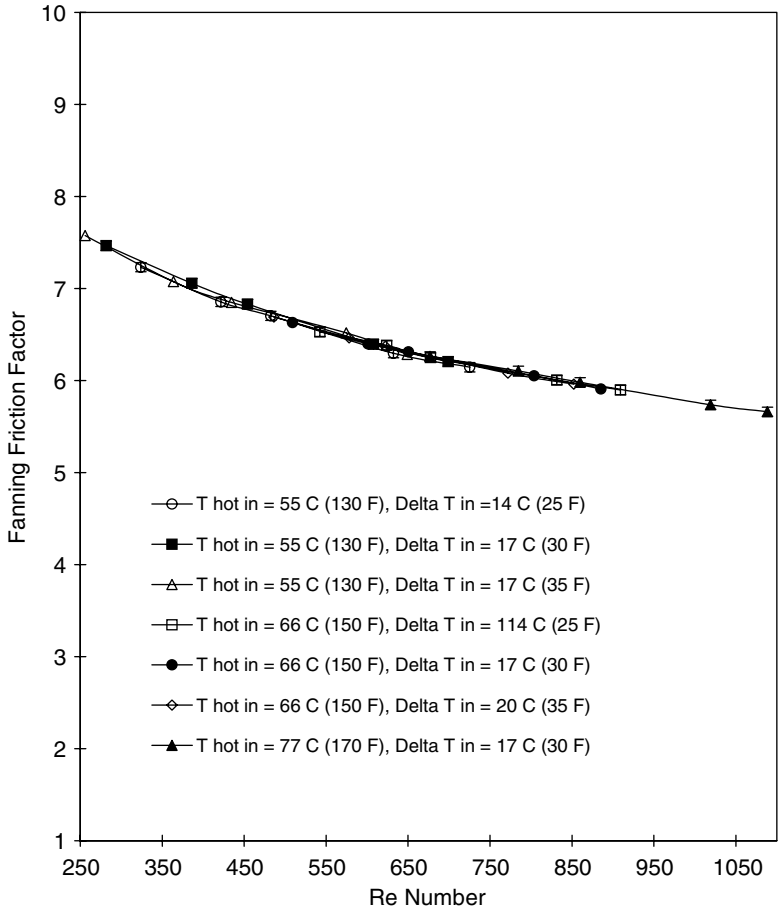

Fig. 14. Effects of Reynolds number on Fanning friction factor of solution at different inlet temperature and varying inlet temperature differences.

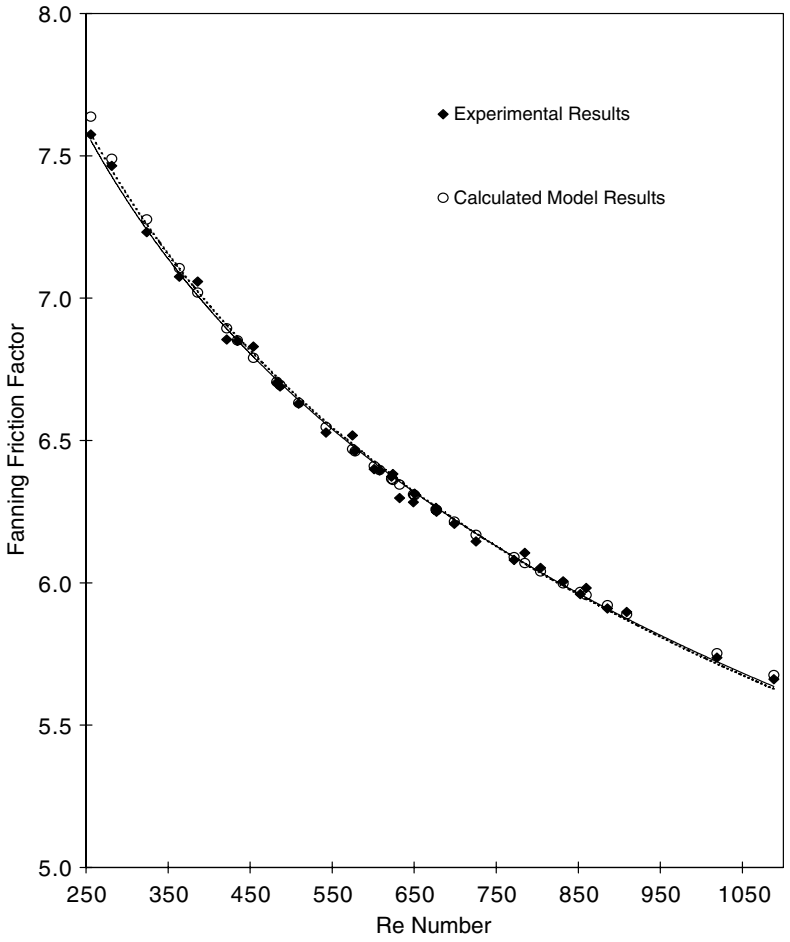

Fig. 15. Comparison of experimental and calculated Fanning friction factors.

When the experimental results at low salt solution temperature are compared with high salt solution temperature, we can clearly see that an undesirable difference of overall heat transfer coefficient at low flow rates. These unpredictable low values for U_{overall} may be due no-flow conditions that can be occurred at the flow passages away from the main streams due to partial crystallization of the solution along those flow passages. In addition, similar behavior of partial crystallization also can be seen in the plots for experimental conditions with higher inlet temperature differences even at high inlet salt solution temperatures.

Since the viscosity of the solution varies significantly with the variation of the temperature, it was shown the overall heat transfer coefficient will increase as the operating temperature increases. When utilizing the heat exchangers with this kind of salt solution, optimization of the plate geometry, especially the included angle between corrugations, theta, will cause a dramatic impact on the performance of the plate heat exchangers.

Acknowledgements

Financial, special, material and technical support given for this work by the Institute of Gas Technology, Gas Research Institute (now combined into the Gas Technology Institute) and the Trane Company is gratefully acknowledged.

References

[1] A. Benbrahim, M. Prevost, R. Bugarel, Performance of a composite absorber, spraying and falling film, in: Proceeding of the International Workshop on Research Activities on Advanced Heat Pumps, Institute of Chemical Engineering, Graz, Austria, October, 1986.
[2] M. Flamensbeck, F. Summerer, P. Riesch, F. Ziegler, G. Alefeld, A cost effective absorption chiller with plate heat exchanger using water and hydroxides, Appl. Thermal Eng. 18 (1998) 413–425.
[3] I. Morioka, M. Kiyota, A. Ousaka, T. Kobayashi, Analysis of steam absorption by a sub-cooled droplet of aqueous solution of LiBr, JSME Int. J., Ser. II 35 (1992) 458–464.
[4] W. Ryan, Water absorption in an adiabatic spray of aqueous lithium bromide solution, Ph.D. Thesis, Illinois Institute of Technology, Chicago, 1995.
[5] F.J. Lawry, Plate type heat exchangers, Chem. Eng. 66 (13) (1959) 89–94.
[6] A.A. McKillop, W.L. Dunkley, Heat transfer in plate heat exchangers, Ind. Eng. Chem. 52 (9) (1960) 740–744.
[7] R.A. Troupe, J.C. Morgan, J. Prifti, The plate heat exchanger – versatile chemical engineering tool, Chem. Eng. Progr. 56 (1) (1960) 124–128.
[8] S. Jenson, Assessment of heat exchanger data, Chem. Eng. Progr. Symp. Ser. 56 (30) (1960) 195–201.

[9] J. Marriott, Where and how to use plate heat exchangers, Chem. Eng. 78 (12) (1971) 127–135.
[10] A. Cooper, Recover more heat with plate heat exchangers, Chem. Eng. 285 (1974) 280–285.
[11] K.S.N. Raju, J.C. Bansal, Design of plate heat exchangers, in: S. Kakac, R.K. Shah, A.E. Bergles (Eds.), Low Reynolds Number Flow Heat Exchangers, Hemisphere Publishing Corporation, 1983 (Chapter 7).
[12] K.S.N. Raju, J.C. Bansal, Plate heat exchangers and their performance, in: S. Kakac, R.K. Shah, A.E. Bergles (Eds.), Low Reynolds Number Flow Heat Exchangers, Hemisphere Publishing Corporation, 1983 (Chapter 7).
[13] M.F. Edwards, Heat transfer in plate heat exchangers at low Reynolds numbers, in: S. Kakac, R.K. Shah, A.E. Bergles (Eds.), Low Reynolds Number Flow Heat Exchangers, Hemisphere Publishing Corporation, 1983 (Chapter 7).
[14] W.W. Focke, J. Zachariades, I. Olivier, The effect of the corrugation inclination angle on the thermohydraulic performance of plate heat exchangers, J. Heat Mass Transfer 28 (8) (1985) 1669–1679.
[15] J. Stasiek, M.W. Collins, M. Ciofalo, P.E. Chew, Investigation of flow and heat transfer in corrugated passages – I. Experimental results, Int. J. Mass Heat Transfer 39 (1) (1996) 149–164.
[16] M. Ciofalo, J. Stasiekand, M.W. Collins, Investigation of flow and heat transfer in corrugated passages – II. Numerical simulation, Int. J. Mass Heat Transfer 39 (1) (1996) 165–192.
[17] R.K. Shah, A.L. London, Laminar Flow Forced Convection in Ducts, Academic Press, New York, 1978.
[18] W.M. Kays, H.C. Perkins, in: W.M. Rohsenow, J.P. Hartnett, E.N. Ganic (Eds.), Hand Book of Heat Transfer Fundamentals, McGraw-Hill, New York, 1985 (Chapter 7).
[19] R.K. Shah, M.S. Bhatti, in: S. Kakac, R.K. Shah, W. Aung (Eds.), Hand Book of Single Phase Convective Heat Transfer, Wiley Inter-Science, New York, 1985 (Chapter 3).
[20] R.A. Buonopane, R.A. Troupe, J.C. Morgan, Heat transfer design methods for plate heat exchangers, Chem. Eng. Progr. 56 (1) (1963) 57–61.
[21] R.D. Crozier, J.R. Booth, J.E. Stewart, Heat transfer in plate and frame exchangers, Chem. Eng. Progr. 60 (8) (1964) 43–45.
[22] D.F. Clark, Plate heat exchanger design and recent development, Chem. Eng. 285 (1974) 275–279.
[23] W.M. Kays, A.L. London, Compact Heat Exchangers, McGraw-Hill, New York, 1984 1988.
[24] C.A. James, R.P. Taylor, B.K. Hodge, The application of uncertainty analysis to cross-flow heat exchanger performance prediction, in: ASME/JSME Thermal Engineering Conference, vol. 4, 1995, pp. 198–207.
[25] N. Epstein, Fouling models: Laminar flow, in: S. Kakac, R.K. Shah, A.E. Bergles (Eds.), Low Reynolds Number Flow Heat Exchangers, Hemisphere Publishing Corporation, 1983 (Chapter 7).